2011 American Control Conference
on O'Farrell Street, San Francisco, CA, USA
June 29 - July 01, 2011

First–Order Short–Range Mover Prediction Model (SRMPM)

Jamahl Overstreet
Dept. of Mechanical & Aerospace Engineering
Polytechnic Institute of NYU
Six MetroTech Center, Brooklyn, NY 11201

Farshad Khorrami
Dept. of Electrical and Computer Engineering
Polytechnic Institute of NYU
Six MetroTech Center, Brooklyn, NY 11201

Abstract— **An important problem for intelligent autonomous mobile systems/agents is the ability to predict the motions of other objects/agents. This has natural extensions to co-operative behavior control, where mobile agents avoid each other by predicting the other's motion. In this paper, we have formulated a spatial probability distribution for moving objects with respect to First-Order predictions, which take into account mobility characteristics and how they relate to probable motion. This is a novel method since the most common approach uses Kalman Filters to estimate future states based upon observed previous states only, assuming a geospatial 2–D Gaussian distribution with monolithic variances in both the normal and tangential directions of motion. Unlike prior approaches, our methodology takes into consideration specific dynamic constraints (e.g., Ackermann Steering), and probable *decision* making capabilities of the mover. By adding higher levels of fidelity to prediction models, more accurate and precise object tracking, avoidance, or engagement can be accomplished with already developed techniques.**

I. Introduction

A major challenge in developing mobile autonomous systems that will coalesce with other autonomous systems, be it organic or mechatronic, is its capacity to predict the actions of its neighbors. As humans, we instinctively navigate around moving objects by estimating the most likely motion another object will make given its mobility characteristics, the environmental influences acting on it (e.g., terrain and weather conditions, neighboring moving objects, traffic rules), and an assumption of the mover's objective (i.e., goals or other motivations). Examples can be of people walking in crowded parks, or driving along highways. In each case, as humans, we track a mover's motions and determine the most likely action it will take, and then we compensate our motions to avoid or engage the other mover. As an example, if we are moving in an area where children are playing, we instinctively know (i.e., expect) that their behavior is more erratic than walking next to elderly people, so we compensate our motions respectively.

For the most part, many intelligent systems such as humans, animals, aquatic and winged vertebrate, know to avoid potential collisions with other mobile objects. This is not always the case as in distracted people or with children who do not know better. Therefore, it is imperative for any autonomous mechatronic system that will move around people, and animals, exhibit obstacle avoidance behaviors. The current state-of-the-art systems are able to avoid stationary objects, and moving objects pose additional challenges.

To avoid or engage dynamic objects, UxVs (Unmanned Ground, Air, Sea/Surface, or Underwater Vehicle) must predict a moving object's future position [1]–[6]. To perform these estimates, Kalman Filters are commonly used to estimate future states based upon previous observed states [7], [8]. For the most part, they assume a geospatial 2–D Gaussian distribution with monolithic variances in both the normal and tangential directions of motion [8]. Some researchers use potential fields to predict the behaviors of objects in the presence of environmental influences [9]. Most of the models do not take into consideration specific dynamic constraints (e.g., Ackermann Steering [10], [11]), nor probable *decision* making capabilities due to environmental influences.

In this paper, we set forth to understand how an *intelligent* object may move on a featureless terrain within a short window of time. We considered this a First–Order Short–Range Mover Prediction Model (SRMPM). This model defines probable motion based upon an initial state (i.e., position, velocity, and curvature), the mobility characteristics of an object (e.g., maximum speed, maximum acceleration, maximum curvature, and Ackermann Steering), and a set of possible trajectories the mover may decide to traverse. As an example, to predict the movements of a small child running in a field, one would use a First–Order SRMPM to characterize his/her motion since the child has not learned the cost of navigating in different terrains and will select paths in uneven terrains with equal probability until he/she learns the amount of effort required to navigate such paths. However, the child has some idea of his/her own capabilities in following paths without falling over.

The focus of this paper is the development of the fundamental algorithmic approach rather than a specific real-time implementation. The authors are performing parallel studies that considers real–time implementation as well as environmental influences.

This paper is organized in the following manner. Section II introduces the concept of multiple orders of SRMPM, and how the First–Order SRMPM fits in to an overall framework. Section III discusses the decision basis from which an intelligent object may select future motions, with an example formulated using kinematically correct equations of motion for ground vehicles. Section IV outlines the formulation of the First–Order SRMPM. Section V shows the simulation

Partial funding for this research was provided by CUNY AGEP at Polytechnic Institute of NYU (Award Number 0450360).

results of the First–Order SRMPM with different initial conditions and prediction time–horizons.

II. Proposed Methodology

Predictions of behaviors are categorized in the following ways, (*i*) the Zeroth–Order SRMPM assumes the object has zero awareness of its surrounding and its capabilities, which is usually modelled using Kalman filters, (*ii*) the First–Order SRMPM assumes the object is unaware of external influences, but is aware of its mobile capabilities (e.g., kinematics and dynamics), (*iii*) the Second–Order SRMPM takes into consideration the surrounding static environmental influences (i.e., terrain, weather, and obstacles), (*iv*) the Third–Order SRMPM takes into consideration the effects of a moving environment, and (*v*) the Fourth–Order SRMPM takes into consideration expected tactical behaviors. In this study, we are laying the groundwork for the First–Order SRMPM.

Our proposed method for determining the mobility profile is based on the following items (given a specific time horizon), (*i*) the formulation of trajectories a mover can navigate given initial conditions, (*ii*) the construction of a decision tree that defines the possible trajectories a mover can take at an instance in time, (*iii*) the concatenation of decision trees at the ends of each trajectory that forms the sampling space of all possible paths, (*iv*) the definition of individual paths based upon the concatenation of trajectories in a sequential order, (*v*) the probability a mover will transition to a trajectory with a certain curvature, given an initial curvature, (*vi*) the probability a mover will be at a specific location along a path given initial conditions, and (*vii*) the probability that a mover will be at a specific cell in the map given the above information and its geometry.

The First–Order SRMPM has the following triplet probabilistic form:

$$(\Omega, \mathcal{A}, \mathbf{P}) \tag{1}$$

where Ω is the sampling space, $\mathcal{A}$ is the algebra of all possible events, and $\mathbf{P}$ is the probability distribution function of event $A \subset \mathcal{A}$. The sampling space is defined as a position in the world map:

$$\Omega = \{\omega : \omega = c_i, i = 1, ..., N_c\}, \tag{2}$$

$$\mathcal{A} = \{A_i : A_i \subset \Omega\}, \tag{3}$$

$$\mathbf{P}(c_i) = \sum_{l=1}^{N_\sigma} \sum_{j=1}^{N_s} \mathbf{P}(c_i|s_j)\,\mathbf{P}(s_j|\sigma_l)\,\mathbf{P}(\sigma_l) \tag{4}$$

$$\mathbf{P}(\sigma_l) = \prod_{k}^{N_O} \mathbf{P}^{(k)}\left(\sigma_l^{(k)}\right) \quad \text{for} \quad k = 0, 1, 2, \ldots \tag{5}$$

where ω is an individual sample of a cell, c_i, that a mover may occupy in the map, N_c is the number of cells in the world map, σ_l is a path the mover may take, s_j is the position of the Gravitational Center (GC) along a path, N_O is the number of prediction orders, N_σ is the number of paths, N_s is the number of states the mover may assume, and k is the index relating to the prediction orders. Equation 5 describes the total probability of path σ_l being selected, which is the product of all prediction order probabilities for selecting σ_l.

III. Decision Tree Formulation

A Decision Basis is defined as a set of probable trajectories a moving object can take given a set of initial conditions. A Decision Tree is formed by concatenating a Decision Basis at the end of each trajectory of a previous Decision Basis. A Tier is the set of decision bases ordered along each path. Tier 1 contains the root Decision Basis, Tier 2 contains the set of decision bases attached to the ends of each trajectory emanating from the Tier 1. Tier 3 is the next set, and so on. The Decision Basis has the following form:

$$\Lambda_T = \bigcup_{i=1}^{N_{\Lambda_T}} \left\{\delta_{(\Lambda_T,i)}\right\}, \quad \text{for} \quad T = 1, 2, \ldots, N_T, \tag{6}$$

where $\delta_{(\Lambda_T,i)}$[1] is the i^{th} trajectory emanating from the Decision Basis Λ_T, N_{Λ_T} is the number of trajectories in the basis Λ_T, and N_T is total number of decision bases.

A path is designated as the following:

$$\sigma_l = \left\{\delta_{l_1}, \delta_{l_2}, \ldots, \delta_{l_{k-1}}, \delta_{l_k}, \delta_{l_{k+1}}, \ldots, \delta_{l_{N_{\delta_l}}}\right\}, \quad \text{for} \quad l = 1, 2, \ldots, N_\sigma, \tag{7}$$

where $\{\delta_{l_k}\}$ is the set of concatenated trajectories that make up σ_l, N_σ is the total number of paths, k is the index of trajectories from the initial position to the final position, N_{δ_l} is the number of trajectories that make up σ_l. Note that the trajectories that are in Λ_T may also be in σ_l.

Figure 1 shows a simple implementation of a Decision Tree. It shows 27 possible paths (N_σ = 27) a mover can select. The first branch (Λ_1) consists of three trajectories $\left(N_{\Lambda_1} = 3, \Lambda_1 = \left\{\delta_{(1,1)}, \delta_{(1,2)}, \delta_{(1,3)}\right\}\right)$, as well as the other decision bases concatenated at the ends of each tier of trajectories. $N_T = 13$, is the total number of decision bases.

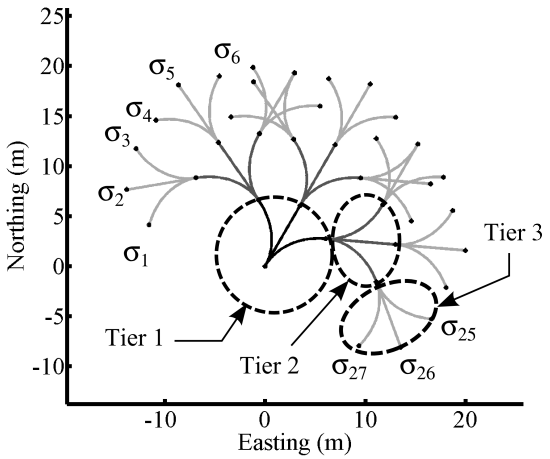

Fig. 1. An example Decision Tree containing 27 possible paths

A. Generating Trajectories

The Decision Tree is a graph that must have a certain amount of fidelity to approximate the infinite possibilities of choices (in direction, speed and time). While in an attempt to satisfy the aforementioned, a balance must be achieved

[1]The subscript Λ_T is removed in following discussion for brevity.

between fidelity and implementability. The more choices embedded in the graph, the longer it takes to compute a solution. Work is being done to determine methods for finding such an optimal balance, but is not discussed here since it is beyond the scope of this topic.

1) Constructing a Simplified Kinematic and Dynamic Model: In order to estimate the actions of moving objects, basic kinematic equations of motion must be formulated. For this paper, we will use a ground vehicle to illustrate the methods. By altering the basic assumptions, the same methodology can be extended to other vehicle types (under water, surface and aerial), as well as gaiting entities such as humans and animals.

The first order predictor looks at variances based upon the capabilities of the mover, such as its physical configuration (size and shape), maximum speed, maximum acceleration, and platform type (biped, quadruped, multi–ped, bicycle/motorcycle, car, truck, tractor). To predict the motions of a mover using a First-Order SRMPM, two primary assumptions have to be made: (*i*) the dynamic and kinematic capabilities and limitations of the mover given a set of initial conditions and constraints (e.g., Ackermann Steering), and (*ii*) the tendencies of a mover without environmental influences.

For this study, the dynamic limitations of the mover are (*a*) the critical trajectory a mover can follow while maintaining stability during a maneuver (Note that for ground vehicles, mobile stability is based upon the marginal state values that tote the conditions for flipping), and (*b*) the maximum distance along a path the mover can take within a specified prediction horizon. It is easy to determine (*b*) since it is the distance the mover can achieve at its maximum acceleration, given its initial velocity. Determination of (*a*) is more involved since it requires finding the maximum curvature rates an object can follow while maintaining stability. To determine non-critical trajectories a mover is likely to follow, the assumption is made that curvature rates will take a mover from an initial curvature to one with a measure of less curvature, since the natural tendencies of a mover's motion is to straighten out rather than continue to increase its curve.

2) Evaluating a Simplified Dynamic Model for Mobile Stability: Here, we consider dynamic stability due to external forces (such as the centrifugal force) that act on an object performing a turn. The flipping is determined by the torque about a tipping point and the associated centrifugal acceleration acting on it, which is greater then the restoring torque about the same point due to gravity. Slipping is an important phenomenon that requires further study, but is outside the scope of this paper. The assumptions made are acceptable, and even conservative, since slipping would aid to an object's stability in regards to the object's tipping parameters.

An example of this can be seen in cars. When the car performs a maneuver that causes the tire to collapse to a geometry that greatly increases the friction between the wheel and the terrain, and prevents the car from sliding, the body behaves as if it was pinned to the ground at that tire. Figure 2(a) shows the simplified model used. The main assumptions used to determine the object's motions are (*i*) the object's motion is evaluated at instantaneous curvatures, (*ii*) the object is traveling at a constant velocity, (*iii*) the Center of Gravity is symmetric about the front width of the object, and (*iv*) there is no slippage between the tires and the terrain.

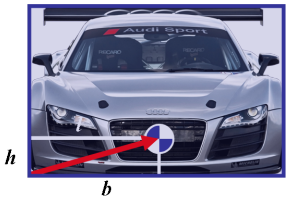

(a) Simplified construct for the Gravitational Center.

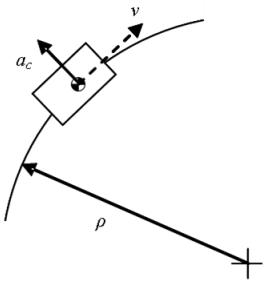

(b) Top view of motion acting on a plane.

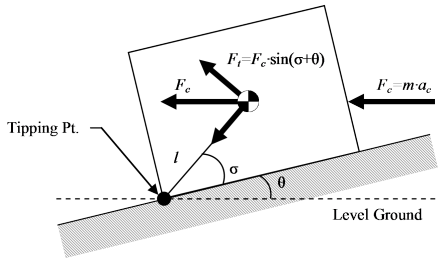

(c) Centrifugal force acting on the side of an object.

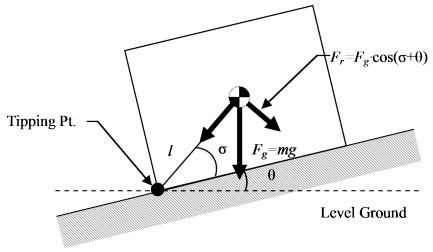

(d) Restoration torque acting at the tipping point.

Fig. 2. Simplified dynamics of a moving object.

Figure 2(c) and Equation 8 depict the forces acting on the simplified model on uneven ground. Figure 2(d) and Equation 10 show the restoration force due to gravity under the same conditions as Figure 2(c). The following equations are the forces and torques acting on the system:

$$F_c = m \cdot a_c = m\frac{v^2}{\rho}, \tag{8}$$

$$\tau_t = F_c \cdot \sin(\sigma+\theta)l = m\frac{v^2}{\rho}\sin(\sigma+\theta)l, \tag{9}$$

$$\tau_r = m \cdot g\cos(\sigma+\theta)l = mg\cos(\sigma+\theta)l, \tag{10}$$

where F_c is the centrifugal force, m is the mass of the object, a_c is the centrifugal acceleration, v is the normal velocity of the object, ρ is the radius of curvature describing the motion, τ_t is the torque generated by F_c, σ is the angle of the CG from the plane of the vehicle relative to the tipping point, θ is the angle of the terrain, l length of the leaver arm from the tipping point to the CG, and τ_r is the restoration torque of due to gravity.

In guaranteeing safe operations, the centrifugal force produced by a turning maneuver has to be less than that of the restoration forces due to gravity, as shown in Equation 11. The constraint equations that restrict flipping are as follows:

$$\tau_t < \tau_r, \tag{11}$$

$$\frac{v^2}{\rho} < g\cot(\sigma+\theta). \tag{12}$$

On a flat surface, $\theta = 0$, resulting in $\cot(\sigma) = b/h$. Therefore the critical instantaneous radius of curvature is

$$\rho_c \triangleq \frac{v^2}{g}\frac{h}{b}. \tag{13}$$

The critical instantaneous radius of curvature dictates the extreme curvatures used in the Decision Basis. Curvatures are not generated that are greater than the critical instantaneous curvature.

IV. Mover Prediction Model

The Probability Distribution Function (PDF) for the First–Order SRMPM is formulated by combining the probabilities that (*i*) an object will most likely transition to paths with instantaneous curvatures that are closer to its current instantaneous curvature, (*ii*) the location of the mover's Center of Gravity (CG) along a chosen path, and (*iii*) its occupation of a cell in the world map given the location of its CG and its physical characteristics.

A. Determining the probability that a mover will transition to a curvature given an initial curvature

A Beta probability density function [12] is used to determine the discrete probability profile associated with the probability that a mover will select a trajectory in an adjoining decision basis, given the termination curvature of its current trajectory. The Beta function is ideal since it skews the higher probabilities of selected trajectories to a group that is closer to the previous trajectory's curvature, as can be seen in Figure 3(a). This figure shows that for the critical curvatures (the extreme left/negative and right/positive curvatures), the probabilities will most likely be zero. Curvatures that are close to the mode, will have higher probabilities (even if they are close to the critical curvature). The following outlines the distribution characteristics of the Beta function used to determine, $\mathbf{P}(\delta_{l_k}|\delta_{l_k-1})$, the conditional probability that a mover navigating along trajectory $\delta_{l_{k-1}}$ will transition to δ_{l_k}, along σ_l. See Equations 6 and 7 for details regarding the relationship between trajectories and paths.

$$\begin{aligned}\mathbf{P}(\delta_{l_k}|\delta_{l_k-1}) =& \frac{1}{B(\alpha^\kappa_{\Lambda_{k-1}}, \beta^\kappa_{\Lambda_{k-1}})} \\ &\times (1-\kappa_{l_k})^{\beta^\kappa_{\Lambda_{k-1}}-1}\kappa_{l_k}^{\alpha^\kappa_{\Lambda_{k-1}}-1}, \qquad (14)\\ &\times \frac{\beta^\kappa_{\Lambda_{k-1}}}{(\alpha^\kappa_{\Lambda_{k-1}}+\beta^\kappa_{\Lambda_{k-1}}+1)}, \qquad (15)\end{aligned}$$

$$I_\kappa(\kappa;\alpha^\kappa_{\Lambda_{k-1}},\beta^\kappa_{\Lambda_{k-1}}) = \frac{B_\kappa(\kappa;\alpha^\kappa_{\Lambda_{k-1}},\beta^\kappa_{\Lambda_{k-1}})}{B(\alpha^\kappa_{\Lambda_{k-1}},\beta^\kappa_{\Lambda_{k-1}})}, \tag{16}$$

$$B(\alpha^\kappa_{\Lambda_{k-1}},\beta^\kappa_{\Lambda_{k-1}}) = \frac{\Gamma(\alpha^\kappa_{\Lambda_{k-1}})\Gamma(\beta^\kappa_{\Lambda_{k-1}})}{\Gamma(\alpha^\kappa_{\Lambda_{k-1}}+\beta^\kappa_{\Lambda_{k-1}})}, \tag{17}$$

$$B_\kappa(\kappa;\alpha^\kappa_{\Lambda_{k-1}},\beta^\kappa_{\Lambda_{k-1}}) = \int_0^\kappa t^{\alpha^\kappa_{\Lambda_{k-1}}-1}(1-t)^{\beta^\kappa_{\Lambda_{k-1}}-1}dt, \tag{18}$$

$$\Gamma(n) = (n-1)!, \tag{19}$$

where κ_{l_k} is the terminating curvature associated with δ_{l_k}, $\beta^\kappa_{\Lambda_{k-1}}$ is the complete beta function, $B_\kappa(\kappa;\alpha^\kappa_{\Lambda_{k-1}},\beta^\kappa_{\Lambda_{k-1}})$ is the incomplete beta function, $I(\alpha^\kappa_{\Lambda_{k-1}},\beta^\kappa_{\Lambda_{k-1}})$ is the regularized complete beta function, $I_\kappa(\kappa;\alpha^\kappa_{\Lambda_{k-1}},\beta^\kappa_{\Lambda_{k-1}})$ is the regularized incomplete beta function, and $\alpha^\kappa_{\Lambda_{k-1}}$ and $\beta^\kappa_{\Lambda_{k-1}}$ are shaping parameters for the Beta distribution of curvature based upon the terminating curvature of the previous trajectory. Figure 3(a) shows an example of a Beta function used to find the probability of a mover selecting the next trajectory.

B. Determining the probability that a mover will select a path

The probability that a path will be selected has the following form:

$$\mathbf{P}(\sigma_l) = \prod_{\delta_{l_k}\in\sigma_l} \mathbf{P}\left(\delta_{l_k}\middle|\bigcup_{\{\delta_{l_j}\in\sigma_l,\delta_{l_j}\prec\delta_{l_k}\}}\{\delta_{l_j}\}\right) \tag{20}$$

where δ_{l_j} precedes δ_{l_i} going from the initial state of the mover to the final state of σ_l. This equation illustrates that the probability that a path σ_l will be chosen is the product of the probabilities that incremental trajectories are chosen along the path, depending upon the conditional probability that adjoining trajectories are selected given their their curvatures, as described in Equation 14.

C. The probability a mover will be at a specific state

To determine the probability that the mover will be at a specific state, $\mathbf{P}(s_k)$, along the path is formulated by

$$\mathbf{P}(s_k) = \sum_l \mathbf{P}(\sigma_l, s_k) = \sum_l \mathbf{P}(s_k|\sigma_l)\mathbf{P}(\sigma_l), \tag{21}$$

$$\mathbf{P}(\sigma_l, s_k) = \mathbf{P}(s_k|\sigma_l)\mathbf{P}(\sigma_l), \tag{22}$$

$$\mathbf{P}(s_k|\sigma_l) = \frac{1}{B(\alpha_l,\beta_l)}(1-s_k)^{\beta_l-1}s_k^{\alpha_l-1}$$

with l being the index of path segments that are a member of path σ_l, and $B(\alpha_l,\beta_l)$ is tuned with respect to physical capabilities of the vehicle (e.g., the initial speeds, maximum achievable speeds, accelerations and braking forces).

D. The probability a mover will be at a specific cell in the map

To determine the probability that the mover will be at a specific state (i.e., cell) in the map, $\mathbf{P}(c_i)$, given the physical dimensions of the mover is formulated using a

normal distribution:

$$\mathbf{P}(c_i) = \sum_k \mathbf{P}(s_k, c_i) = \mathbf{P}(c_i|s_k)\mathbf{P}(s_k), \tag{23}$$

$$\mathbf{P}(c_i|s_k) = \frac{1}{\sqrt{2\pi\sigma_n\sigma_t}} e^{-\left\{\frac{(s_k^n-\mu_n)^2}{2\sigma_n^2} + \frac{(s_k^t-\mu_t)^2}{2\sigma_t^2}\right\}} \tag{24}$$

where c_i is a cell in the map, $\mathbf{P}(s_k, c_i)$ is the joint probability of the mover's GC at state s_k and some part of the mover's body occupying cell c_i (where s_k^n and s_k^t are the components of s_k transformed into normal and tangential components, respectively, to the direction of the mover). Figure 3(b) shows the method of discretizing the continuous probability density function, $\mathrm{P}(s)$, into a probability distribution function, $\mathrm{P}_D(s_k)$, for each state (s_k) along the entire path, spanning multiple tiers of trajectories.

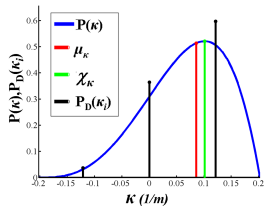

(a) The probability of a mover choosing a trajectory at a decision node. μ_κ is the mean, and χ_κ is the mode.

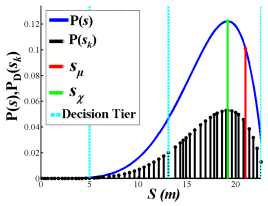

(b) The probability of a mover being along a path (the path is comprised of contiguous trajectory segments). s_μ is the mean, and s_χ is the mode.

Fig. 3. Using the Beta Function for determining the probability of a mover traversing to different trajectories and its state along a trajectory.

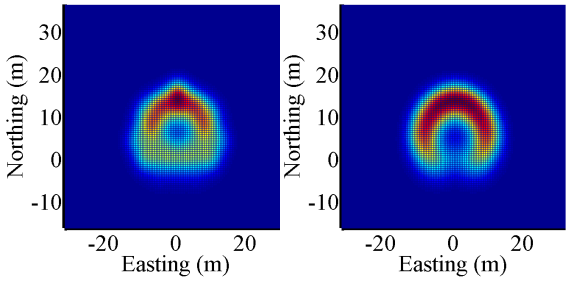

(a) $\Lambda_T = 7$, $\tau = 4\ s$ (b) $\Lambda_T = 11$, $\tau = 4\ s$

(c) $\Lambda_T = 7$, $\tau = 3\ s$ (d) $\Lambda_T = 11$, $\tau = 3\ s$

Fig. 4. Model fidelity comparison between $\Lambda_T = 7$ and $\Lambda_T = 11$.

V. Simulation Results

The characteristic probability profiles generated in this paper show that the profiles are more similar to waves than ellipses. The monotonic variances in 2–D spatial Gaussian approximations do not take into consideration possible curvatures that objects may take. Different model fidelities are constructed by adding more trajectories to each decision basis. The finer the discretization (i.e., the more trajectories in a basis), the more accurate the model.

1) Case 01: This case refers to a situation where the initial speed of an object traveling due North is at 4 m/s with zero curvature (i.e., the object is moving straight). Figure 4 shows the results of this case using two different fidelity models. The left profiles consist of $\Lambda_T = 7$ and the right profiles consist of $\Lambda_T = 11$. For a Decision Tree containing 7–dimensional uniform decision bases, spanning 3 and 4 seconds, and has 343, and 2,401 paths, respectively. A Decision Tree containing 11–dimensional uniform decision bases, spanning 3 and 4 seconds, and has 1,331 and 14,641 paths.

It can be seen in these figures that decision bases with greater numbers of paths create smoother profiles. Figure 4 shows that the model with lower dimension decision bases has a grainier profile, and it shows that $\Lambda_T = 7$ has the highest probabilities concentrated at a single point due North of the object. In contrast, Figure 4 shows the probabilities with $\Lambda_T = 11$ has a more distinctive horseshoe shape, where the higher probabilities are smoothed out along an arc. By inspection, Figures 4(a) - 4(d) show that a 2–D Gaussian approximation degrades with large time horizons.

It can also be seen that the probable motion of the mover propagates like a wave emanating from its initial position. The Gaussian model does not capture this wave like distribution. This is the case since most Gaussian approximations do not take into consideration possible curvatures the object may take. As can be seen in Fig. 4(a) and 4(b), the highest Northern probable location for the mover is at $d \cong s_o \cdot t$ (the distance is approximately equal to the initial speed multiplied by the time, with out acceleration).

2) Case 02: This case refers to a situation where the initial speed of an object is traveling due North at 4 m/s, with an initial left curvature of -0.050 $1/m$. As in the previous case, Figure 5 shows two different fidelity models ($\Lambda_T = 7$ and $\Lambda_T = 11$). Similar to Case 01, the profile with the least number of possible paths to select becomes more grainy. The figures with $\Lambda_T = 7$ show a high probability that the object will go due North. This is a residue from the coarseness of the discretized space. As seen in Figure 5, the Decision Basis with the higher dimension show a smoother profile with the higher probabilities condensed toward the left. This is intuitively obvious since an object will try to maintain its initial motion (within a finite time) given no other influences. The Gaussian models are unable to capture this characteristic.

3) Case 03: This case refers to a situation where the initial speed of an object is traveling due North at 8 m/s with zero curvature (seen in Figure 6). The figure shows that

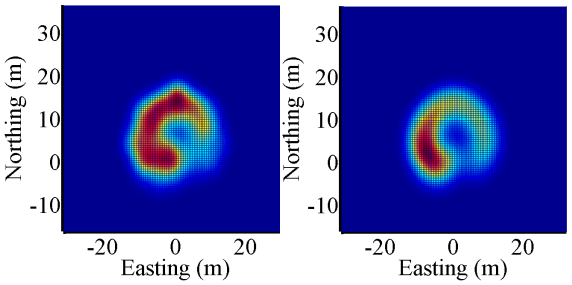

(a) $\Lambda_T = 7$, $\tau = 4\ s$ (b) $\Lambda_T = 11$, $\tau = 4\ s$

(c) $\Lambda_T = 7$, $\tau = 3\ s$ (d) $\Lambda_T = 11$, $\tau = 3\ s$

Fig. 5. Model fidelity comparison between $\Lambda_T = 7$ and $\Lambda_T = 11$.

with higher dimensional decision bases, the expected location (i.e., mode of the distribution) is more focused due North, but the profile maintains a horseshoe shape, and the probable motion propagates like a wave. A Decision Tree containing 15–dimensional uniform decision bases, spanning 3 and 4 seconds, and has 3,375 and 50,625 paths, respectively. This case shows that as the number of trajectories in the decision bases increases, there most likely is an optimum number of trajectories to use, where by increasing the number of trajectories beyond this limit does not greatly add to the fidelity of the model.

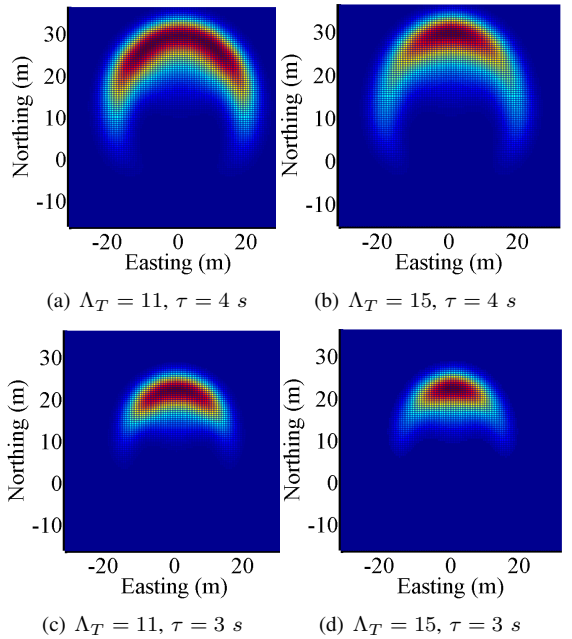

(a) $\Lambda_T = 11$, $\tau = 4\ s$ (b) $\Lambda_T = 15$, $\tau = 4\ s$

(c) $\Lambda_T = 11$, $\tau = 3\ s$ (d) $\Lambda_T = 15$, $\tau = 3\ s$

Fig. 6. Model fidelity comparison between $\Lambda_T = 11$ and $\Lambda_T = 15$.

VI. Conclusion

In conclusion, this paper sets forth the ground work to construct a First–Order SRMPM that can accurately predict future positions of an intelligently moving object, given its initial conditions and the absence of environmental influences. This construct is beneficial since it has a higher level of fidelity than those of a 2–D Gaussian distributions, which are generated with little to no insight into actual mobile capabilities and decision processes of intelligent objects.

The proposed method is a better approximation than a 2–D Gaussian probability distribution since the Gaussian distribution has monolithic directional variances along the normal and tangential directions of motion. This study allows researchers to use the methods outlined in this paper as a benchmark to evaluate the accuracy of other methods for constructing mover probability profiles. Through the insights gain in this paper, analytical and numerical methods can be constructed to approximate the shapes of the First–Order SRMPM PDFs, which would be more applicable for real–time implementation.

Further studies are being preformed to construct higher levels of prediction models that take into consideration environmental influences, such as static and dynamic objects, as well as goals and expected behaviors. The authors are applying these techniques to their obstacle avoidance methods for UxV research and development.

References

[1] P. Krishnamurthy and F. Khorrami, "GODZILA: A low-resource algorithm for path planning in unknown environments," in *Proceedings of the 2005 American Control Conf.*, vol. 48, pp. 357–356, Mar. 2007.

[2] P. Krishnamurthy, F. Khorrami, and T. L. Ng, "A hierarchical path planning and obstacle avoidance system for an autonomous underwater vehicle," in *Proceedings of the 2009 American Control Conference*, (St. Louis, MO), July 2009.

[3] P. Krishnamurthy, F. Khorrami, and T. L. Ng, "Obstacle avoidance for unmanned sea surface vehicles: hierarcal approach," in *Proceedings of the 2008 International Federation of Automatic Control Conference*, (Seoul, Korea), July 2008.

[4] A. Foka and P. Trahanias, "Predictive autonomous robot navigation," in *Proceedings of the IEEE/RSJ 2002 International Conference on Intelligent Robots and Systems*, vol. 1, pp. 490–495, Oct. 2002.

[5] A. Foka and P. Trahanias, "Predictive control of robot velocity to avoid obstacles in dynamic environments," in *Proceedings of the 2003 IEEE/RSJ International Conference on Intelligent Robots and Systems*, vol. 1, pp. 370–375, Oct. 2003.

[6] A. Elnagar and A. Hussein, "An adaptive motion prediction model for trajectory planner systems," in *Proceedings of the 2003 IEEE International Conference on Robotics and Automation*, vol. 2, pp. 2442–2447, Sept. 2003.

[7] R. Jiang, X. Tian, L. Xie, and Y. Chen, "A robot collision avoidance scheme based on the moving obstacle motion prediction," in *ISECS 2008 International Colloquium on Computing, Communication, Control, and Management*, vol. 2, pp. 341–345, Apr. 2008.

[8] C. Prevost, A. Desbiens, and E. Gagnon, "Extended kalman filter for state estimation and trajectory prediction of a moving object detected by an unmanned aerial vehicle," in *Proceedings of the 2007 American Control Conference*, pp. 1805–1810, July 2007.

[9] C. Fulgenzi, C. Tay, A. Spalanzani, and C. Laugier, "Probabilistic navigation in dynamic environment using rapidly–exploring random trees and gaussian processes," in *Proceedings of the IEEE/RSJ 2008 International Conference on Intelligent Robots and Systems*, pp. 1056–1062, Sept. 2008.

[10] J. Ackermann, "Robust control prevents car skidding," *IEEE Control Systems Magazine*, vol. 17, pp. 23–31, June 1997.

[11] J. Ackermann, J. Guldner, W. Sienel, R. Steinhauser, and V. Utkin, "Linear and nonlinear controller design for robust automatic steering," *IEEE Transactions on Control Systems Technology*, vol. 3, pp. 132 – 143, Mar. 1995.

[12] http://www.itl.nist.gov/div898/handbook/eda/section3/eda366h.htm.